Received: 14 October 2017 | Revised: 21 July 2018 | Accepted: 30 August 2018

DOI: 10.1111/jfr3.12490

CIWEM Chartered Institution of Water and Environmental Management | Journal of Flood Risk Management | WILEY

ORIGINAL ARTICLE

Three-dimensional hydraulic characterisation of the Arno River in Florence

Cosimo Peruzzi* | Marco Castaldi | Simona Francalanci | Luca Solari

Department of Civil and Environmental Engineering (DICEA), University of Florence, Florence, Italy

Correspondence
Cosimo Peruzzi, Department of Civil and Environmental Engineering (DICEA), University of Florence, Via di Santa Marta 3, Florence, Italy.
Email: cosimo.peruzzi@polito.it

***Present address**
Department of Environment, Land and Infrastructure Engineering (DIATI), Polytechnic of Turin, Corso Duca degli Abruzzi 24, Turin, Italy.

Rivers in historical cities, such as the Arno River in Florence, are typically characterised by unique complex-shaped hydraulic structures (such as bridges and weirs). The flow interaction with these structures can lead to a fully 3D flow field which cannot be properly investigated with commonly employed 1D, and even 2D, hydraulic models. Nowadays, 3D computational fluid dynamics (CFD) tools can be successfully used in river management context. Florence is characterised by a high risk of flooding and the disastrous consequences of such events being greatly increased due to its inestimable artistic heritage. The main cause of flooding is the limited hydraulic conveyance capacity of the Arno River in Florence due to several complex hydraulic structures along the reach. The present work represents the first 3D hydraulic model of the Arno River in the urban reach of Florence. The geometric model was created using the 3D bed topography of the river surveyed in 2015. The hydraulic model was calibrated and validated using discharge and water stage field data measured in 2016. The 3D model can be used as a more realistic tool for exploring mitigation solutions for the reduction of hydraulic risk.

KEYWORDS
flood damages, flood mitigation, hydraulic modelling, hydraulic structures

1 | INTRODUCTION

Florence has suffered from the effects of urban flooding of the Arno River since its foundation; 56 floods are recorded since 1177 (Arno River Basin Authority, 1996). The last extreme flood in chronological order is the event that occurred on November 4, 1966, which had worldwide resonance considering the damage caused both in terms of human lives and to its historical heritage (Figure 1). The maximum flow discharge was estimated at roughly 4,200 m^3/s (Caporali, Rinaldi, & Casagli, 2005). The return period of the 1966 flood event was approximated to be in the range of 150–200 years (Arrighi, Brugioni, Castelli, Franceschini, & Mazzanti, 2013).

Immediately following the 1966 flood, people from all over the world came to Florence to help with rescuing and limiting the damage to over a million books and almost one thousand paintings, frescoes, and sculptures (Alexander, 1980). Flood risk management became a leading-edge topic following this catastrophic event.

Since the 1966 flood, the Arno River in Florence has been the subject of few hydraulic studies. The first numerical model that simulates the propagation of flooding in the Arno River basin upstream of Florence was proposed by Panattoni and Wallis (1979). The two most prominent studies modelling the hydraulics on the Arno River through the city of Florence were the physical scale model of the University of Bologna by Cocchi (1972, 1975) and the 1D numerical model developed by Settesoldi, Paris, and Lubello (1996). Cocchi (1972, 1975) built the model of the urban reach of the Arno River with a fixed and mobile bed using cross sections surveyed in the 60s. The purpose of the studies of

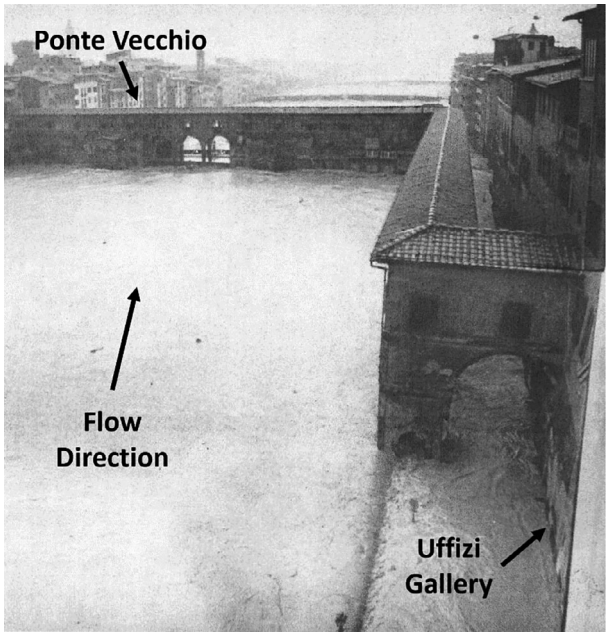

FIGURE 1 Photo of Ponte Vecchio and the Uffizi Gallery in Florence during the flood of November 4, 1966. Upstream view (source: Principe & Sica, 1967)

Cocchi was to investigate possible structural strategies for increasing the maximum conveyance capacity of the Arno River. These studies indicated that the maximum conveyance capacity of the urban reach increased from 3,090 to 3,450 m^3/s (with no safety allowance) with the lowering by 1 m of the aprons of both Ponte Vecchio and the Santa Trinita bridges. The lowering of the aprons was initiated in 1977 (Canfarini, 1984). Settesoldi et al. (1996) developed a 1D steady flow model based on the finite difference method to solve the basic equations of continuity and momentum; they investigated an 8.5 km long reach of the Arno River, from the Rovezzano weir (upstream Florence) to the Cascine weir (downstream Florence). This model predicted that the initiation of flooding could be expected at a flow discharge of 3,200 m^3/s.

Importantly, the current maximum safe discharge that can be contained within the banks appears to be well below the maximum discharge that was observed during the 1966 event. Therefore, 50 years after the 1966 flood, Florence still remains at high hydraulic risk, as pointed out by the International Technical and Scientific Committee (ITSC) in their final report (Galloway et al., 2017). This report describes the current status of flood protection for Florence and identifies steps that could be taken to reduce the current flood risk. Especially, the ITSC points out the necessity of conducting laboratory experiments in tandem with three-dimensional hydrodynamic modelling to assess the rating curves for the hydraulic structures of the Arno River and to better understand its hydraulic characteristics.

The uncertainty of these hydraulic characteristics comes as a direct consequence of the complexity of the hydraulic structures (i.e., historical arch bridges and oblique weirs) on the Arno River in Florence. The interaction of the flow with arch bridges and oblique weirs is a typical complex 3D process characterised by the presence of secondary flow cells which cannot be reproduced with 1D and 2D models. Modelling these interactions is of relevance to provide a realistic estimation of the discharge coefficients and the energy losses of these structures and thus, of the conveyance capacity of the River.

In the last decade, an always greater number of 3D computational fluid dynamics applications were conducted with the scope of understanding the flow interaction with hydraulic structures commonly present in a river; recent examples include: flow over a spillway (Dargahi, 2006), flow of bottom outlets with moving gates (Dargahi, 2010; Haun, Olsen, & Feurich, 2011), backwater profiles due to bridges (Kocaman, 2014), and turbulent flow fields inside fishways (Quaranta, Katopodis, Revelli, & Comoglio, 2017).

This work presents the first three-dimensional modelling of the Arno River using a CFD tool (Flow Science Inc., 2015). The aim is to obtain better insight into the 3D hydraulic behaviour of the Arno River and its interaction with hydraulic structures. In fact, the flood protection of historical cities, such as Florence, should be based on a more realistic understanding of the flow behaviour. In this sense 3D models of short urban river reaches should be regarded as a significant tool in a modern flood protection approach to optimise flood risk reduction actions by means of both structural and nonstructural interventions.

Relevant modelling results about the Arno River are presented in this work. They include: discharge coefficients and energy losses of hydraulic structures, rating curves, and flow characteristics at the Santa Rosa oblique weir. Importantly, these results can be incorporated in simplified and widespread used 1D models to obtain a more robust physics-based interpretation of the hydraulics.

2 | MATERIALS AND METHODS

The present work is focused on a 1,303 m long reach of the Arno River, located in the urban part of Florence. This reach is bound by the upstream and downstream cross sections AR0584 and AR0559, respectively (Figure 2). Moving downstream, the following five hydraulic structures can be found: Ponte Vecchio, Santa Trinita bridge, Alla Carraia bridge, Santa Rosa weir, and the Amerigo Vespucci bridge. The Uffizi gauge station, the unique water level gauge station in the city centre, is located just upstream of Ponte Vecchio. The Santa Rosa weir has an angle of 51° in respect to channel axis and its crest has a slope of $3.22 \cdot 10^{-3}$ toward the right-hand side.

The input information includes geometric and hydraulic data. The geometric data used to create both the river bed

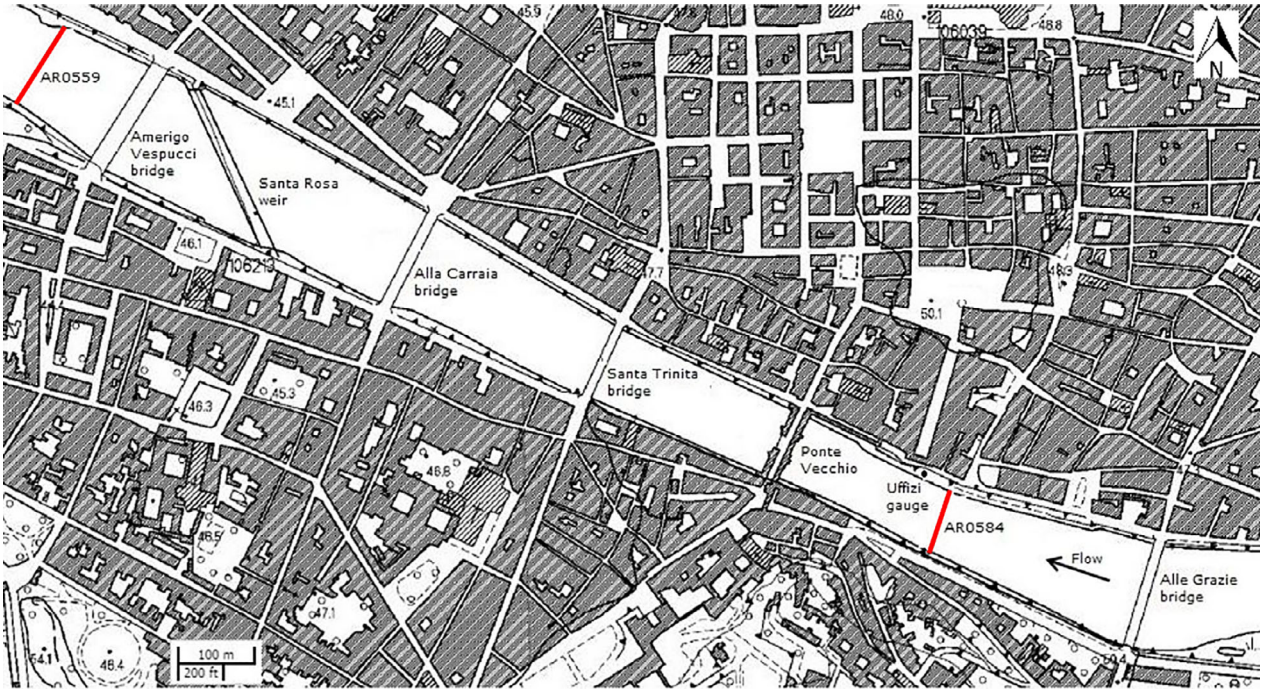

FIGURE 2 Studied reach of the Arno River in the city centre of Florence. Red lines indicate the upstream (AR0584) and downstream (AR0559) cross sections. There are four bridges (Ponte Vecchio, Santa Trinita, Alla Carraia, and Vespucci) and an oblique weir (Santa Rosa)

topography and the hydraulic structures were obtained from two sources: (a) the cross sections surveyed in 2000 (Arno River Basin Authority[1]) and (b) the three-dimensional bed topography surveyed in 2015 using multibeam sonar technology (Firenze 2016 project[2]). Figure 3 provides an overview of the studied reach bed topography.

The hydraulic data included experimental, simulated, and field data. Experimental and simulated data were derived from the results obtained by Cocchi (1972) and Settesoldi et al. (1996), respectively. The field data were measured, within the framework of the Firenze 2016 project, during the time period December 30, 2015–February 16, 2016 (Francalanci, Paris, Solari, & Federici, 2016): flow discharges were measured at Alle Grazie bridge (about 315 m upstream from the Uffizi gauge) for five different conditions, while at the same time water level measurements were conducted upstream and downstream of the four bridges within the study reach. Water levels were measured by means of a plumb line and a laser distance meter. Flow discharges at Alle Grazie bridge were estimated by means of flow velocity measurements taken along a given vertical by using a current meter (see Francalanci, Paris, & Solari, 2013 for details). The values of water level and discharge measurements are summarised in Table 1: the first two measured data correspond to low flow conditions, while the others refer to higher flows; these data represent valuable and unique input for calibration and validation of the numerical model. The uncertainties of discharge measurements are due to the unsteadiness of the flow and the time required for collecting the field data. In the present case, a total of nine verticals were employed to minimise the errors associated to flow unsteadiness while ensuring the accuracy of the measurements (Francalanci et al., 2013).

The study method consisted of numerical simulations using the software FLOW-3D. FLOW-3D is based on the finite volume method (FVM) to solve the full Reynolds-Averaged Navier–Stokes (RANS) equations of fluid motion in Cartesian coordinates (Flow Science Inc., 2015). FVM involves the division of the computational domain into volumes and the imposition of conservation laws to these volumes. In FLOW-3D the geometry of solid elements and the position of free surfaces are represented through the Fractional Area/Volume Obstacle Representation (FAVOR™) and the volume of fluid (VOF) techniques, respectively. FAVOR™ is a powerful method for incorporating the geometry effects into the governing equations through the definition of fractional area and volume variables. More details on the VOF model are reported in Nichols and Hirt (1975) and in Hirt and Nichols (1981).

The numerical model was set up in several steps, that is, creation of the geometry (CAD model) and computational grid, definition of initial and boundary conditions and model sensitivity analyses.

The solid geometry of the urban reach was created using AutoCAD (Figure 4). The riverbed topography was obtained

[1]http://www.adbarno.it/opendata/?page_id=204&nf=Arno
[2]http://toscana.firenze2016.it/en/

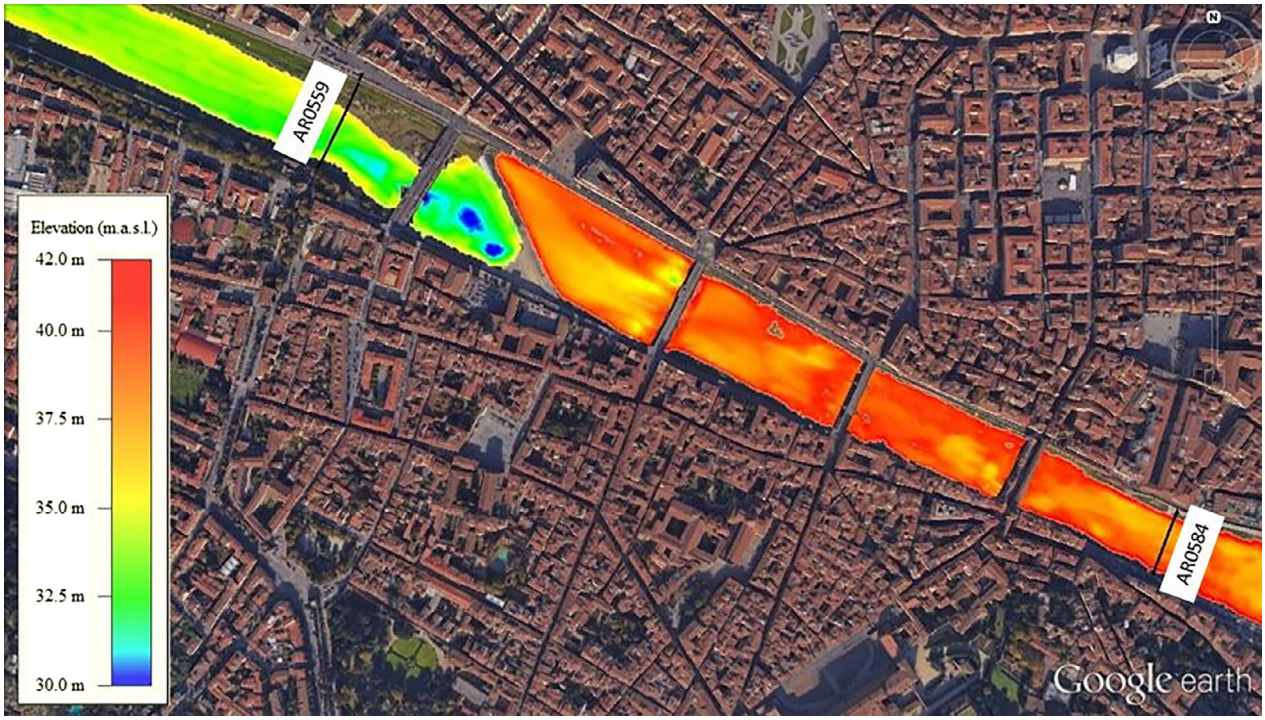

FIGURE 3 The 3D bed topography of the Arno River surveyed in 2015 in the city centre of Florence with indication of the boundary cross-sections (AR0584 and AR0559). Note the drop of about 8 m across the Santa Rosa weir

TABLE 1 Free surface elevation and discharge measurements during the period of December 2015–February 2016. Results of the scale model by Cocchi (1972) are included

Location	30/12/15	12/01/16	15/01/16	15/02/16	16/02/16	Scale model
	Free surface elevation (m a.s.l.)					
Ponte Vecchio upstream	41.44	41.73	42.08	42.33	43.42	44.01
Ponte Vecchio downstream	41.45	41.71	42.058	42.30	43.51	44
Santa Trinita bridge upstream	41.41	41.67	42.06	42.26	43.14	43.68
Santa Trinita bridge downstream	41.34	41.72	42.03	42.24	43.09	43.67
Alla Carraia bridge upstream	41.37	41.61	41.99	42.14	42.97	43.43
Alla Carraia bridge downstream	41.36	41.67	42.01	42.13	42.86	43.4
Amerigo Vespucci bridge upstream	36.43	36.89	37.53	37.94	39.60	-
Amerigo Vespucci bridge downstream	36.32	36.72	37.60	37.85	39.58	-
	Discharge (m^3/s)					
Alle Grazie bridge	9.6	63.8	250	321	909	800

from the 3D bed topography surveyed in 2015 (Figure 3), while the riverbanks and hydraulic structures were created using the 2000 survey.

The simulations were carried out using a multiblock non-uniform structured mesh. This mesh was composed with two different rectangular mesh-blocks. The former covered the entire model geometry and had a cell size of 1 m in the x-direction, 1 m in the y-direction and 0.5 m (28 cells) or 1 m (10 cells) along the z-direction; the mesh along the z-direction was refined to properly represent the riverbed. Overall, the number of mesh cells in (x, y, z) was of $1{,}301 \times 176 \times 38$ corresponding to a total of 8,701,088 cells. The latter mesh had cubic cells of 0.5 m with a total number of 3,755,520 cells and it was placed only across the Santa Rosa weir to have a greater resolution of the small flow depths over this structure at low discharge values. Furthermore, the use of this finer grid was more appropriate for reproducing the shape of the weir.

Figure 5 compares the CAD model and its visualisation by FLOW-3D for the nonuniform Cartesian mesh.

A total number of six steady-state simulations were done, calibration and validation included. Upstream inlet boundary conditions were volume flow rate and the corresponding water level, for each simulation, while the hydrostatic pressure was set as the outlet boundary condition at the end of the reach. The bottom and the levees were defined as no-slip conditions. Atmospheric pressure was considered for the water surface. Table 2 summarises all the simulations that were carried-out together with the upstream and downstream boundary conditions.

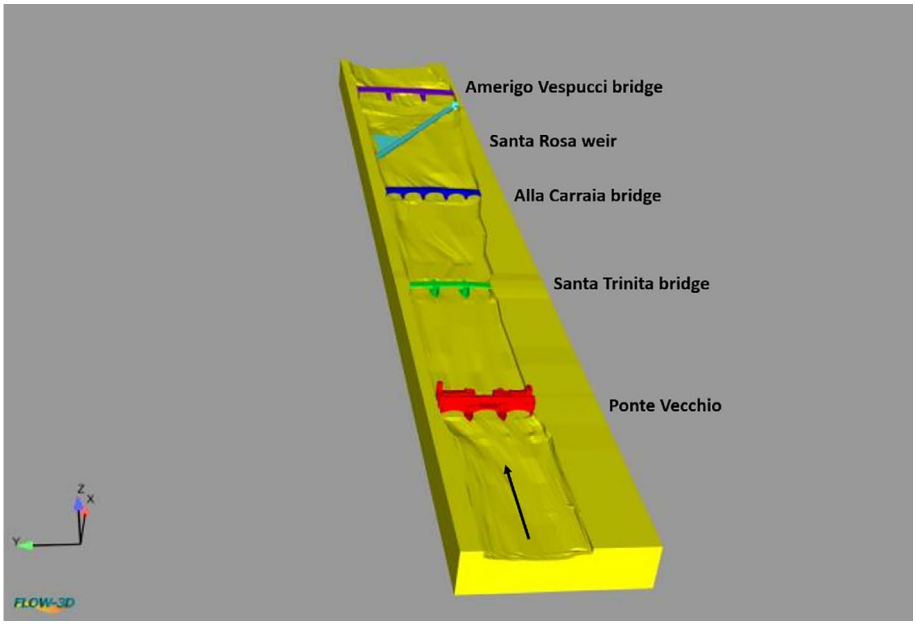

FIGURE 4 CAD model of the modelled urban reach

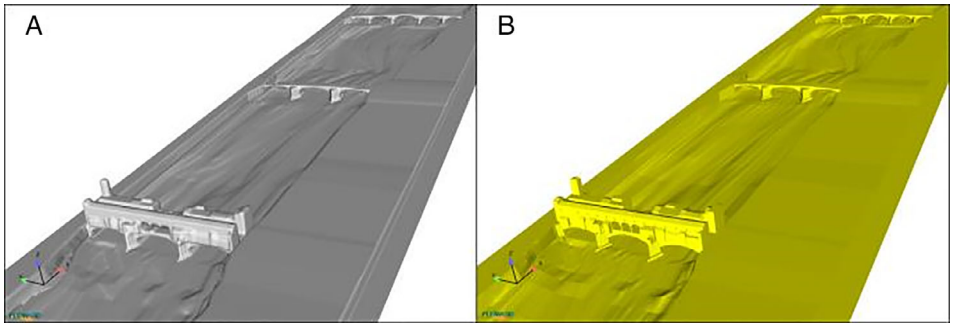

FIGURE 5 Comparison between: FLOW-3D resolution (a); CAD model (b)

TABLE 2 Boundary conditions for the computational fluid dynamics simulations

Type	Discharge (m^3/s)	Water level	
		Upstream (m a.s.l.)	Downstream (m a.s.l.)
Calibration	250	42.16	37.60
Validation	909	43.82	39.58
Simulation 1	800	44.24	39.34
Simulation 2	1,400	45.47	41.33
Simulation 3	2,200	46.68	43.51
Simulation 4	3,000	48.11	45.41

In the model calibration and validation, the upstream flow discharge boundary conditions and the downstream water level boundary conditions were taken from the measured field data of Table 1. The upstream water levels were taken from the values recorded by the Uffizi hydrometer for the same period of time as the field data measurements.

In the subsequent model simulations (1–4), the upstream boundary conditions (volume flow rates and water levels) were taken from the study of the University of Bologna by Cocchi (1972), assumed to be probably the most reliable hydraulic study with high flow discharges. The downstream water level boundary conditions were instead estimated from steady-state 1D HEC-RAS (Hydrologic Engineering Centers - River Analysis System; Brunner, 2010) simulations run using the same flow discharges as in FLOW-3D simulations. The reach of the Arno River used in the HEC-RAS simulations had the same extension as the CAD model. The boundary conditions used in the HEC-RAS simulations were the water level and the energy line slope as upstream and downstream boundary conditions, respectively. This procedure was necessary as the scale model of the University of Bologna was shorter and no other data were available.

A single fluid region covering the entire model was set as initial condition to decrease the computational time required for a simulation to reach the steady-state.

The simulations were done using the generalised minimum residual method (GMRES). GMRES is the FLOW-3D default implicit numerical solver that is highly accurate and efficient for a wide range of cases (Flow Science Inc., 2015). The first order of approximation of the Taylor's expansion was used for all the simulations. Furthermore, the influence on the solution of the following variables was investigated:

1. Hydraulic resistance by defining three different regions with appropriate Manning's roughness coefficients that is, riverbed, banks, and hydraulic structures.
2. Influence of turbulence model that is, k-ε and renormalisation group (RNG) models.
3. Grid dependency of results.

More than 50 simulations were done to test the model and to obtain mesh-independent solutions. A simulation time of 840 s was set for each simulation as it was sufficient for the CFD model to reach numerical stability. Convergence is reached when changes in solution variables from one iteration to the next are negligible, overall property conservation is achieved or when quantities of interest have reached steady values. The computing time required for one run was about 3–4 days using a personal computer (RAM 16 GB, processor i7-6700HQ). It is worth noticing that in FLOW-3D the total hydraulic head is computed assuming that the streamlines are parallel. In this work, due to the strongly three-dimensional flow, this parameter was not used. To overcome this issue, baffles were added as flux surfaces. Baffles, which were simply a diagnostic function and did not affect the flow, provided data on volume flow rate, flux-averaged hydraulic head, and wetted area. The wetted areas obtained through the baffles were involved in the procedure for evaluating discharge coefficients of hydraulic structures. The discharge coefficient C_d is a fundamental variable that is commonly used in hydraulic analyses to include the overall effects of contraction, turbulent losses, nonuniform distribution of velocity, and nonhydrostatic pressure distribution. With reference to Figure 6, the general expression of C_d for a bridge is (Chow, 1959):

$$C_d = \frac{C_c}{\sqrt{\alpha + k_e + k_p}} \tag{1}$$

in which C_c and α are the contraction and energy coefficients, respectively at a section downstream of the bridge, k_e is a coefficient that accounts for eddy losses due to turbulence, and k_p is a coefficient for the nonhydrostatic distribution of pressure.

The discharge coefficients of the urban reach bridges were estimated directly from FLOW-3D results in accordance with the following procedure. Two cross-sections were selected, one far upstream to the bridge, where uniform flow was attained (numbered 0 in Figure 6) and the other within the contraction zone, in correspondence of the vena contracta (numbered 1 in Figure 6). As FLOW-3D solves RANS equations, it was assumed that the ratio between the wetted area of the contracted section 1 and the wetted area of section 0 directly provided the discharge coefficient. Following this assumption, the C_d value of each bridge was obtained. The discharge coefficients were then corrected with the energy coefficient values. In particular, the energy coefficient α was varied in the range 1.05–1.35. The upper limit of α was estimated by numerically integrating, using the Cavalieri-Simpson's rule, the velocity profiles that diverged from the theoretical logarithmic law profile.

C_d values of the Santa Rosa weir were estimated from Aichel's formula (Aichel, 1953) since it is applicable in the case of oblique weirs with respect to the main flow direction:

$$Q = \frac{2}{3} C_d B_w \sqrt{2g} h_w^{\frac{3}{2}} \sec(\varphi) \tag{2}$$

in which B_w is the channel width, φ is the weir angle, g is the gravitational acceleration and h_w is the piezometric head above the weir.

3 | RESULTS AND DISCUSSIONS

3.1 | Model calibration and validation

The calibration process involved the following parameters: the cell size of meshes, the turbulence model and the Manning's roughness coefficients. No major flooding events have occurred since the 2015 survey and thus the riverbed was considered to be in a state of dynamic equilibrium. Good reproduction of solid boundaries and a reasonable computing time were the aspects involved in mesh cell size choice. The limited availability of CPUs did not allow for further refinement of the grid size. Several simulations were done using both the standard two equations $k - \varepsilon$ (Launder & Spalding, 1972) and the RNG models (Yakhot & Orszag, 1986; Yakhot, Orszag, Thangam, Gatski, & Speziale, 1992). The RNG model provided a better agreement with the field data. In fact, as pointed out by Speziale and Thangam (1992), one major difference between the $k - \varepsilon$ and the RNG models is that the latter does not require specially-made wall damping functions but can be directly integrated toward a solid edge. This allows for better representation of separated and curved flows, which are typical situations in open-channel flow. Its improved performance is highlighted by many works on natural rivers (Bradbrook, Biron, Lane, Richards, & Roy, 1998; Bradbrook, Lane, & Richards, 2000; Dargahi, 2004; Hodskinson & Ferguson, 1998). The choice of Manning's roughness coefficients represents the most significant element in model calibration (Morvan, Knight, Wright, Tang, & Crossley, 2008). The CAD model was divided into three parts, that is, the riverbed, the riverbanks, and the hydraulic structures in order to allow the allocation of differing roughness coefficients. The values of roughness used were: $n = 0.032$ s/m$^{1/3}$ for the riverbed, $n = 0.03$ s/m$^{1/3}$ for the banks, and $n = 0.026$ s/m$^{1/3}$ for the hydraulic structures. The result of the model calibration is displayed in Figure 7 in which the field data are dated January 15, 2016. The profile of the free water surface was extracted from the centerline of the urban reach as was also done for the field data. The results were taken along a longitudinal section having a normalised position y_N (i.e., the position in the spanwise direction y, measured from the inner right side of AR0584 cross section, divided by its width) of 0.57.

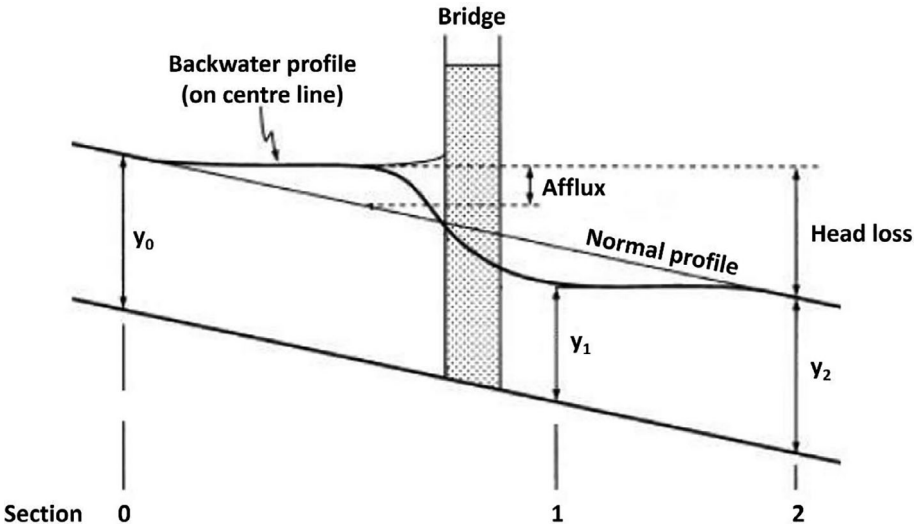

FIGURE 6 Water profile variation at a bridge (source: modified from Hamill, 1999)

The root-mean-square error (RMSE) was 0.092 m. The percentage error referred to the mean water depth was 2.4%.

The model validation ensures that flow parameters adjusted in the model calibration are suitable for predicting a new set of field data. The model validation was achieved using the same parameters defined in the model calibration process that is, cell size, turbulent model, and Manning's roughness coefficients. The results are shown in Figure 8 at a y_N of 0.57. The field data were collected on February 16, 2016.

The RMSE was 0.119 m and the percentage error referred to the mean water depth was of 2.3%. Thus, the model was successfully calibrated and validated.

3.2 | Results

The results obtained from the flow simulations were used to extract various hydraulic properties of the urban reach and its hydraulic structures, that is, water levels, discharge coefficients, streamlines, energy losses, and the rating curve at the Uffizi gauge station.

3.2.1 | Water levels

Figure 9 displays the free surface elevation profiles at a discharge of 3,000 m^3/s; the results for the remaining discharges have a similar trend, hence are not shown here for the sake of brevity. The free surface elevation profiles were taken for normalised positions y_N of 0.21, 0.57, and 0.91.

The slopes and shapes of the profiles change along the reach as well as in the transversal direction, due to the strong three-dimensionality of the flow. In particular, under the Ponte Vecchio bridge the surface elevation in the centreline position (green line) is about 0.40–0.60 m below the water levels on the sides (blue and red line); the Santa Trinita bridge shows an asymmetric behaviour with the water level on the right side (blue line) below the water level on the left side (red line), this is due to large scour holes that can be

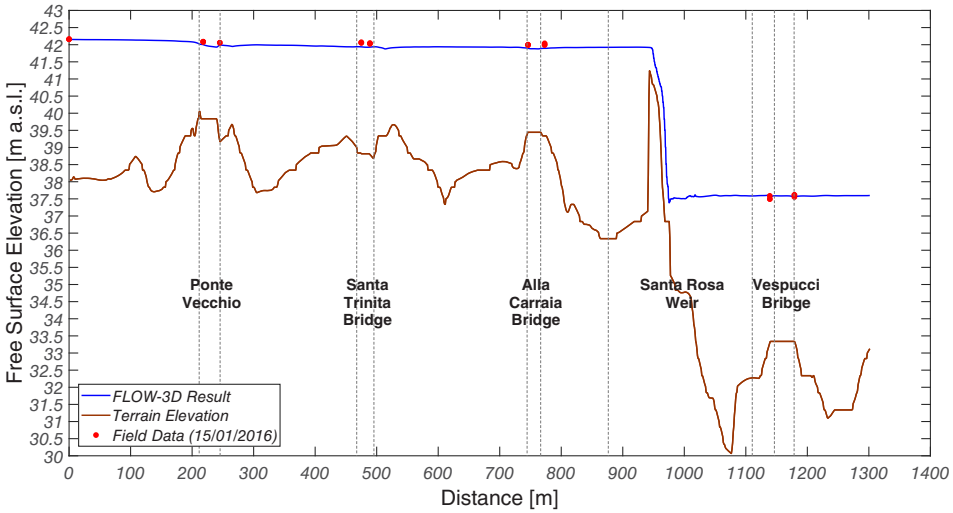

FIGURE 7 Model calibration: Comparison between model predicted water levels and field data (red points are field measurements taken on January 15, 2016)

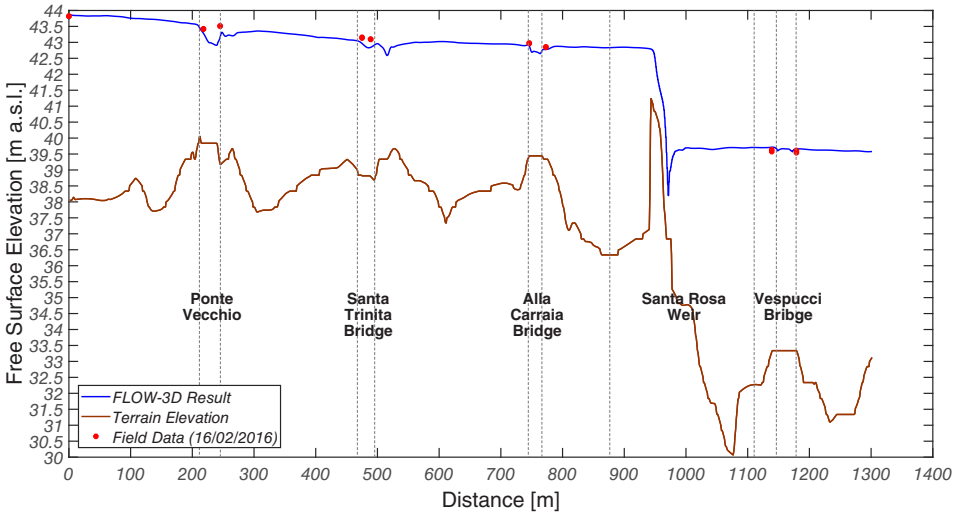

FIGURE 8 Model validation: Comparison between model water levels and field data (red point are field measurements taken on February 16, 2016)

observed downstream of the Vespucci bridge piers. Furthermore, Figure 9 shows a discrepancy between the simulated FLOW-3D results and those used as comparison, namely the scale model by Cocchi (1972) and the 1D hydraulic model by Settesoldi et al. (1996). In particular, water levels in the urban reach used as comparison seem to be overestimated, but this trend can be presumably ascribed to the fact that both the scale and numerical models are not calibrated with direct field measurements. This can be also seen in Table 1 where water levels in the scale model at a discharge of 800 m^3/s appear to be higher than field data for the discharge of 909 m^3/s collected on February 16, 2016. This discrepancy can also be considered a consequence of possible riverbed changes that can have a significant impact on water levels. Moreover, in the scale model by Cocchi the reproduced bed roughness was quite large thus producing higher water levels that might have resulted in an increased safety factor (Galloway et al., 2017). The disagreement between FLOW-3D and the 1D hydraulic model by Settesoldi et al. (1996) can instead be explained by the fact that the latter was affected by discharge coefficients at the hydraulic structures which were not known at the time. Figure 10 shows the 3D flow depth at a discharge of 3,000 m^3/s.

In the present work, it was evaluated the minimum distance z_0 between the free water surface and the top of the levees at a discharge of 3,000 m^3/s, which is the critical point for the safety of the city. It is important to highlight that z_0 was always lower at the right side with respect to the flow direction. The minimum distance of 0.89 m was detected downstream of the Amerigo Vespucci bridge (Figure 11).

Moreover, the flow regime across the hydraulic structures is given in Table 3; according to Hamill (1999), the flow under a bridge is type 1 in a submerged condition, type 4 in case of subcritical flow, type 5 in case of weak supercritical flow, and type 6 in case of supercritical flow. Regarding a weir, the flow regime can be either free (F) or submerged (S) depending on whether the flow passes through the critical depth or not (Skogerboe, Hyatt, & Lloyd, 1967).

It should be noted that the Santa Rosa weir is characterised by a partly free and partly submerged flow at a

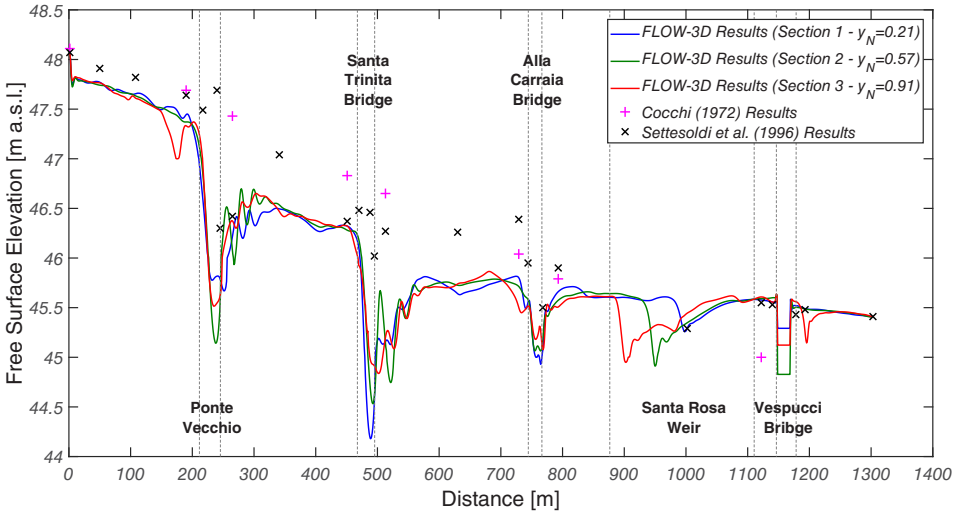

FIGURE 9 Free surface elevation at a discharge of 3,000 m^3/s

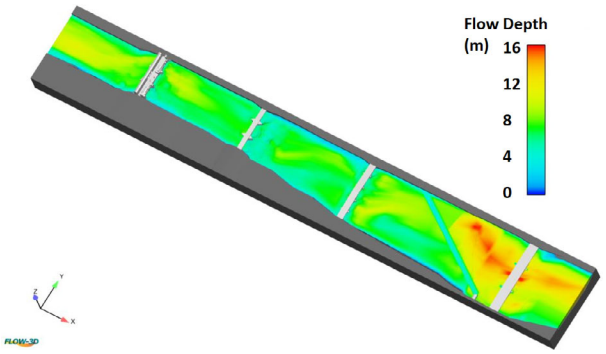

FIGURE 10 3D configuration of the flow depth at a discharge of 3,000 m^3/s (top view, flow from left to right)

discharge of 2,200 m^3/s (Figure 12). The change of its flow regime occurs at a normalised position y_N of 0.16 and is caused by the transverse slope of its crest; the flow is submerged on the right-hand side (S-type) and free on the left side (F-type). Importantly, the weir is submerged for higher flow discharges thus suggesting that water levels in the urban reach are controlled by a boundary condition which is located further downstream of the weir.

Furthermore, the entire urban reach is characterised by a more or less accentuated transverse slope of the water levels. In particular, this slope is directed toward the right-hand side due to the fact that the urban reach is part of a weak channel meander. The mean difference in height between water levels at the left and right-hand sides Δz can be estimated following the formula (Graf & Altinakar, 1998):

$$\Delta z = \frac{B_w r}{r_1 r_2} \frac{V^2}{2g} \tag{3}$$

in which B_w is the channel width, r is the radius of curvature of the meander, V the mean velocity of the flow, r_1 and r_2 are the radii of curvature of the concave and convex banks, respectively, and g is the gravitational acceleration. At a flow discharge of 3,000 m^3/s, Δz was about 22.7 mm. This mean value conforms well with the mean value obtained through the simulation, although some local zones (such as in proximity of Ponte Vecchio and Alla Carraia bridge) of the river are characterised by a transverse slope in the opposite direction and of significantly higher value. The slopes in these zones are attributable to local phenomena due to the presence of the hydraulic structures and to local bed variations.

3.2.2 | Discharge coefficients

The discharge coefficients C_d allow a direct comparison of the hydraulic behaviour of the various structures. The ranges of C_d obtained are listed in Table 4.

It appears that Ponte Vecchio has the lowest C_d in comparison with the other bridges, thus it offers the strongest blockage to the flow. Regarding the Santa Rosa weir, the discharge coefficients variation is based on the flow condition over the weir. Values of $C_d \approx 0.7$ are typical of the free flow condition and $C_d \approx 0.45$ are typical of the submerged flow condition. Moreover, the bridge C_d were compared at a discharge of 3,000 m^3/s with the corresponding values obtained by applying the United States Geological Survey (USGS) method; this method was developed through laboratory investigations by Kindsvater, Carter, and Tracy (1953) and later extended by Matthai (1967). This comparison is illustrated in Table 5.

The values estimated with the USGS-method correspond to the upper limit of ranges obtained with the simulations (Table 4), except for Ponte Vecchio where C_d is greatly overestimated. The reason being that Ponte Vecchio is a massive and complex-structured bridge that strongly interacts with the flow, generating hydraulic effects that only a 3D CFD analysis is able to reproduce. The quantification of the discharge coefficients is extremely important because every historical bridge is unique and thus in 1D simulations appropriate coefficients should be used instead of generic reference values.

3.2.3 | Streamlines at the oblique weir of Santa Rosa

The complexity of the flow field across the oblique weir of Santa Rosa can be seen in Figure 13, which illustrates the streamlines pattern at an elevation of around 42.5 m a.s.l. at a discharge of 3,000 m^3/s (totally submerged situation).

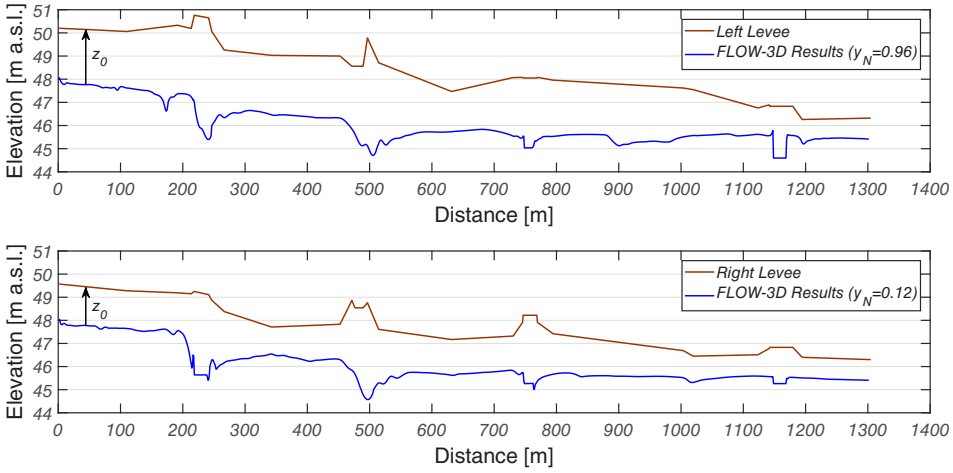

FIGURE 11 Difference in elevation between the water levels and top of the walls at 3000 m^3/s

TABLE 3 Different flow regime types across the hydraulic structures (1 submerged, 4 subcritical, 5 weak supercritical, 6 supercritical, F free flow at a weir, S submerged flow at a weir)

Hydraulic structure	800 m^3/s	1,400 m^3/s	2,200 m^3/s	3,000 m^3/s
Ponte Vecchio	4	4/5	5/6	5/6
Santa Trinita bridge	4	4	5/6	5/6
Alla Carraia bridge	4	4	4/5	4
Santa Rosa weir	F	F	F/S	S
Amerigo Vespucci bridge	4	4	4	1

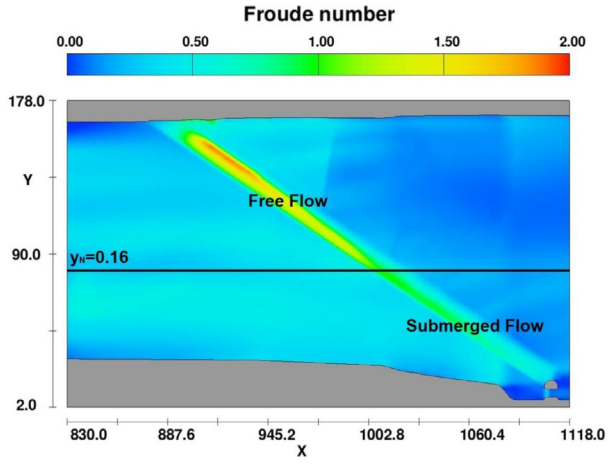

FIGURE 12 Flow regime over the Santa Rosa weir at a discharge of 2,200 m^3/s (top view, flow from left to right)

While the more-common weirs perpendicular to channel axis gives rise to a downstream 2D flow pattern, in the case of oblique weirs, the streamlines are deviated due to the presence of secondary flow cells and thus the flow is 3D. This finding is in analogy with previous laboratory experiments (Tuyen, 2006). Importantly, the Santa Rosa weir produces an accumulation of streamlines on the left pier of the immediately downstream Amerigo Vespucci bridge. This is a possible explanation for the huge local scour which was detected during the 2015 bed survey.

3.2.4 | Energy losses

The calculation of the energy losses was done directly using FLOW-3D results (Table 6) by means of baffles placed in proximity of the hydraulic structures.

Table 6 shows that Ponte Vecchio produces the highest energy losses while the lowest energy losses are produced by the Amerigo Vespucci bridge. Regarding the Santa Rosa weir, in case of submerged flow condition, the energy losses are lower than those calculated for the free flow condition. The energy losses at discharges of 800 and 1,400 m^3/s are a consequence of the difference in water elevation between upstream and downstream of the weir (i.e., loss of potential energy). Furthermore, as might be expected, the energy losses produced by the presence of the bridges increase by augmenting the discharge while the Santa Rosa weir displays the opposite result.

3.2.5 | Rating curve

The rating curve was calculated close to the location of the Uffizi hydrometer (AR0583.5 cross-section). Figure 14 compares the rating curve obtained with FLOW-3D with that elaborated by the Hydrological Regional Service (SIR) at the Uffizi hydrometer. In addition, the figure displays the field data reported in Francalanci et al. (2016). The field data were surveyed in the period January 31, 2014–February 16, 2016. Each dataset was produced in the following way: the real discharge was measured downstream of Alle Grazie bridge (at about 315 m upstream of the Uffizi hydrometer) while the water level was simultaneously recorded by the Uffizi hydrometer.

The FLOW-3D rating curve is compatible with the field data at discharges up to 1,000 m^3/s, but it slightly overestimates the water levels for higher discharges. This observation cannot be inferred at extremely high discharges, since there are no measurements above 1,300 m^3/s. In general, it can be noted that the FLOW-3D rating curve matches the 2016 measured data better than the 2014 measured data. The corresponding RMSE are of 0.024 and of 0.372 m, respectively. This better agreement with the 2016 measured data is probably due to the fact that the CFD simulations used a bed topography surveyed in 2015 and no important flooding events occurred before the monitoring campaign of 2016. Moreover, the measurements in 2014 were carried out during the falling limb of the level hydrograph which showed a much higher peak value, such that flow irregularity played a significant role. Finally, the comparison between the two available topographies of 2000 and 2015 showed a weak depositional trend, which is aligned with the dissimilarity between the two datasets.

TABLE 4 Discharge coefficients of hydraulic structures

Hydraulic structure	C_d (−) 800 m^3/s	C_d (−) 1,400 m^3/s	C_d (−) 2,200 m^3/s	C_d (−) 3,000 m^3/s
Ponte Vecchio	0.52–0.59	0.5–0.57	0.49–0.56	0.49–0.55
Santa Trinita bridge	0.83–0.94	0.75–0.85	0.63–0.71	0.61–0.69
Alla Carraia bridge	0.65–0.74	0.64–0.73	0.61–0.69	0.64–0.73
Santa Rosa weir	0.67–0.76	0.68–0.69	0.48–0.68	0.44–0.47
Amerigo Vespucci bridge	0.72–0.81	0.74–0.84	0.75–0.85	0.73–0.83

TABLE 5 Coefficient of discharge values estimated with USGS method (second column) and the mean values obtained from the CFD simulations (third column)

Hydraulic structure	C_d (−) 3,000 m^3/s (USGS-method)	C_d (−) 3,000 m^3/s (mean value)
Ponte Vecchio	0.75	0.52
Santa Trinita bridge	0.69	0.65
Alla Carraia bridge	0.72	0.68
Amerigo Vespucci bridge	0.82	0.78

Abbreviations: CFD, computational fluid dynamics; USGS, United States Geological Survey.

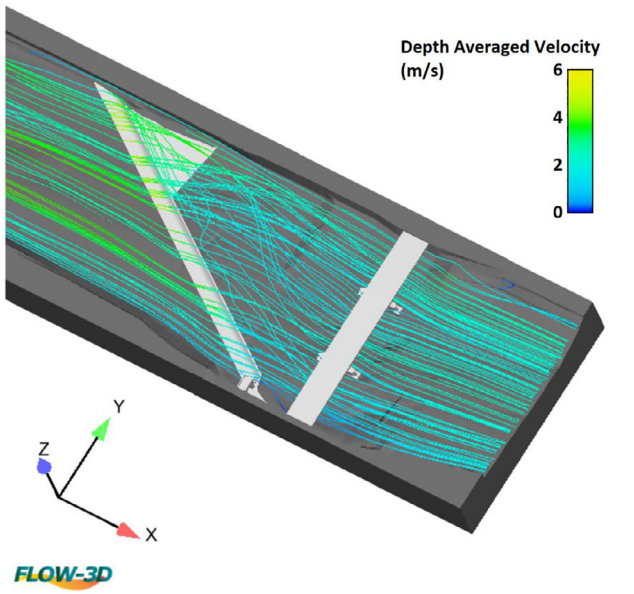

FIGURE 13 Details of the streamlines pattern at a discharge of 3,000 m^3/s across the oblique weir of Santa Rosa. The streamlines are coloured by the value of depth-averaged velocity (top view, flow from left to right)

TABLE 6 Total energy losses across hydraulic structures

Hydraulic structure	ΔH (m) 800 m^3/s	ΔH (m) 1,400 m^3/s	ΔH (m) 2,200 m^3/s	ΔH (m) 3,000 m^3/s
Ponte Vecchio	0.3	0.42	0.52	0.54
Santa Trinita bridge	0.19	0.32	0.48	0.49
Alla Carraia bridge	0.07	0.13	0.18	0.19
Santa Rosa weir	2.92	1.87	0.71	0.35
Amerigo Vespucci bridge	0.05	0.07	0.07	0.08

4 | CONCLUSIONS AND SUGGESTIONS

The present study concerns the first application of a CFD three-dimensional model to the urban reach of Arno River in Florence. The model was successfully calibrated and validated by means of field data measured upstream and downstream of each bridge within the study reach during the period of December 30, 2015–February 16, 2016. Four CFD simulations with constant flow discharge were performed. These allowed us to obtain an improved hydraulic characterisation of the Arno River reach. The main conclusions are as follows:

1. Along the entire urban reach, the minimum distance between the water surface and the top of the walls is always on the right-hand side of the river with respect to the flow direction. At a discharge of 3,000 m^3/s its value is 0.89 m and occurs downstream of the Amerigo Vespucci bridge.
2. Ponte Vecchio and the Santa Trinita bridges are characterised by supercritical flows at discharges of 2,200 m^3/s or higher. The other bridges are always characterised by a subcritical flow. The Amerigo Vespucci bridge is fully submerged at a discharge of 3,000 m^3/s at both its upstream and downstream sections. The Santa Rosa weir is characterised by two hydraulic regimes that is, submerged or free flow. At a discharge of 3,000 m^3/s the Santa Rosa weir is fully submerged.
3. The ranges of the calculated discharge coefficients are: 0.49–0.59 for Ponte Vecchio, 0.61–0.94 for the Santa Trinita bridge, 0.61–0.74 for Alla Carraia bridge, 0.44–0.76 for the Santa Rosa weir, and 0.72–0.85 for the Amerigo Vespucci bridge.
4. The interaction of the flow with the complex river structures (such as arch bridges and oblique weirs) is fully three-dimensional. A more realistic interpretation of the hydraulics of these structures therefore requires a 3D modelling approach.
5. Ponte Vecchio is a massive bridge and it produces the highest energy losses while the lowest energy losses are produced by the Amerigo Vespucci bridge. Ponte Vecchio produces energy losses in the range 41–49% of the total head loss produced by all the bridges together, while the losses due to Amerigo Vespucci bridge are only in the range 6–8% of the total. The Santa Rosa weir produces between 83 and 66% of the total energy losses at discharges of 800 and 1,400 m^3/s, respectively; these losses are due to the free flow condition.
6. Rating curves upstream and downstream of Ponte Vecchio and upstream of the Santa Rosa weir were obtained. In particular, the rating curve upstream of Ponte Vecchio has RMSE values of 0.372 and of 0.024 m in comparison to the field measurements of 2014 and 2016, respectively.

The present study is a relevant step towards a full and realistic hydraulic characterisation of the Arno River, being the first three-dimensional study of its urban reach. Such progress was possible thanks to the intense field monitoring activity that was developed within the Firenze 2016 project, in particular by means of a detailed 3D river bed survey which allowed for the first-ever creation of a 3D geometrical model of the Arno River in Florence.

Importantly, the CFD analysis of the river pointed out that the Santa Rosa weir plays a crucial role in the control of the outflow in the city centre of Florence. Changes to the

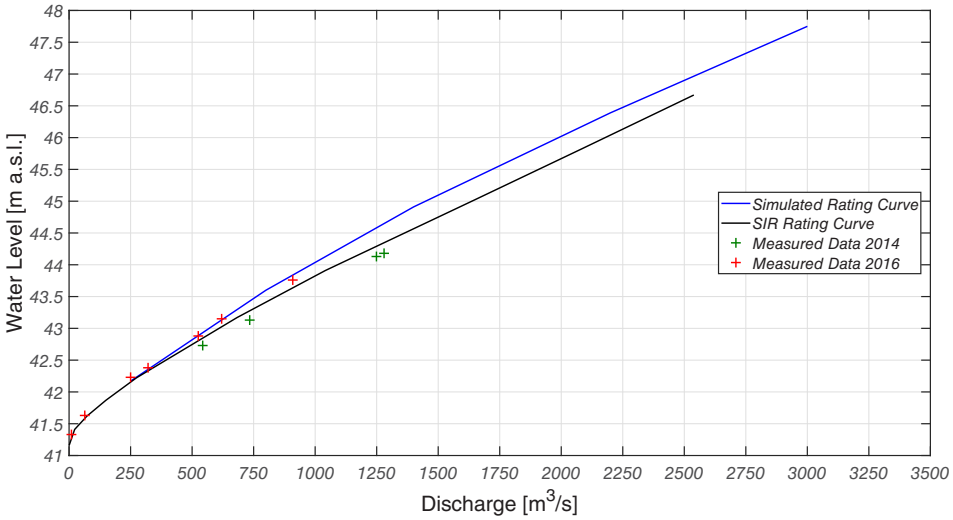

FIGURE 14 Comparison between the FLOW-3D and the SIR rating curves

weir shape or other modifications should be studied as a possible flood risk countermeasure. For instance, a 1 m lowering of the Santa Rosa weir crest was briefly investigated and it produced a decrease in water levels of about 0.2 m at a discharge of 3,000 m^3/s. However, the lowering of the weir crest would probably produce a riverbed degradation and consequently a probable water levels reduction greater than 0.2 m.

3D hydraulic simulations are therefore required to obtain a more realistic interpretation of the flow field when complex hydraulic structures (arch bridges as Ponte Vecchio or oblique weirs as Santa Rosa) are present. 3D numerical models, if properly calibrated and validated with field data, may be then employed by the competent flood management authorities for exploring new solutions for the reduction of the hydraulic risk.

ACKNOWLEDGEMENTS

The authors are thankful to professors Bijan Dargahi (KTH Royal Institute of Technology) and Enio Paris (University of Florence) for their many comments and suggestions. The Editor, the Associate Editor, and three anonymous Reviewers are gratefully acknowledged for their useful comments.

The authors confirm the absence of any conflict of interest that might have influenced the authors' objectivity within this study.

ORCID

Cosimo Peruzzi https://orcid.org/0000-0002-1418-9575
Marco Castaldi https://orcid.org/0000-0003-4523-1278
Simona Francalanci https://orcid.org/0000-0002-6013-2203
Luca Solari https://orcid.org/0000-0001-9227-4305

REFERENCES

Aichel, O. G. (1953). Abflusszahlen für schiefe weher [Discharge ratios for oblique weirs]. *ZVDI*, *95*(1), 26–27 (in German).

Alexander, D. (1980). The Florence floods – What the papers said. *Environmental Management*, *4*(1), 27–34.

Arno River Basin Authority (1996), *Piano di Bacino del Fiume Arno: Rischio Idraulico [The hydraulic risk plan for the Arno River]*. Pisa: Periodico di Informazione dell'Autorità del Bacino del Fiume Arno, 5 Quaderni (in Italian).

Arrighi, C., Brugioni, M., Castelli, F., Franceschini, S., & Mazzanti, B. (2013). Urban micro-scale flood risk estimation with parsimonious hydraulic modelling and census data. *Natural Hazards and Earth System Sciences*, *13*, 1375–1391.

Bradbrook, K. F., Biron, P. M., Lane, S. N., Richards, K. S., & Roy, A. G. (1998). Investigation on secondary circulation in a simple confluence geometry using a three-dimensional numerical model. *Hydrological Processes*, *12*(8), 1371–1396.

Bradbrook, K. F., Lane, S. N., & Richards, K. S. (2000). Numerical simulation of three-dimensional, time-averaged flow structure at river channel confluences. *Water Resources Research*, *36*(9), 2731–2746.

Brunner, G. W. (2010). *HEC-RAS River Analysis System Hydraulic User's Manual*. Version 4.1. Davis, CA: Hydrologic Engineering Center.

Canfarini, A. (1984). La esecuzione del ribassamento delle platee dei ponti Vecchio e Santa Trinità [On the lowering of the aprons of bridges Ponte Vecchio and Santa Trinita]. *Bollettino degli Ingegneri*, *3*, 3–11 (in Italian).

Caporali, E., Rinaldi, M., & Casagli, N. (2005). The Arno River flood. *Giornale di Geologia Applicata*, *1*, 177–192.

Chow, V. (1959). *Open-channel hydraulics*. New York, NY: McGraw-Hill Civil Engineering Series.

Cocchi G. (1972). *Studio su modello idraulico del regime di piena del fiume Arno entro la città di Firenze, nel tratto compreso tra il ponte Alle Grazie e la traversa S. Rosa [Technical report on the hydraulic model of the lowered aprons of bridges Ponte Vecchio and Santa Trinita: Fixed bed experiments]*, Hydraulic Institute University of Bologna (in Italian).

Cocchi G. (1975*). Studio su modello idraulico a fondo mobile delle escavazioni prodotte da eventi di piena nel fiume Arno in corrispondenza del Ponte Vecchio e del ponte S. Trinità [Technical report on the hydraulic model of the lowered aprons of bridges Ponte Vecchio and Santa Trinita: Mobile bed experiments]*, Hydraulic Institute University of Bologna (in Italian).

Dargahi, B. (2004). Three-dimensional flow modelling and sediment transport in the River Klarälven. *Earth Surface Processes and Landforms*, *29*(7), 821–852.

Dargahi, B. (2006). Experimental study and 3D numerical simulations for a free-overflow spillway. *Journal of Hydraulic Engineering*, *132*(9), 899–907.

Dargahi, B. (2010). Flow characteristics of bottom outlet with moving gates. *Journal of Hydraulic Research*, *48*(4), 476–482.

Flow Science Inc. (2015). *FLOW-3D user manual release 11.1*. Santa Fe, NM: Flow Science.

Francalanci, S., Paris, E., & Solari, L. (2013). A combined field sampling-modeling approach for computing sediment transport during flash floods in a gravel-bed stream. *Water Resources Research*, *49*, 6642–6655.

Francalanci S., Paris E., Solari L., Federici G. V. (2016). *Monitoraggio e Idraulica del Tratto Urbano del Fiume Arno a Firenze [Monitoring and hydraulics of the city centre reach of the Arno River in Florence]*. In *Proceedings, XXXV Convegno Nazionale di Idraulica e Costruzioni Idrauliche*, Bologna, pp. 899–902 (in Italian).

Galloway, G., Seminara, G., Blöschl, G., Garcia, M., Montanari, A., & Solari, L. (2017). *Saving a world treasure: Protecting Florence from flooding*. Vol. 115. Firenze: Firenze University Press. http://www.fupress.com/catalogo/saving-a-world-treasureprotecting-florence-from-fooding/3517

Graf, W. H., & Altinakar, M. S. (1998). *Fluvial hydraulics: Flow and transport processes in channels of simple geometry*. Chichester: John Wiley and Sons.

Hamill, L. (1999). *Bridge hydraulics*. New York, NY: E & FN SP.

Haun, S., Olsen, N. R. B., & Feurich, R. (2011). Numerical modeling of flow over trapezoidal broad-crested weir. *Engineering Applications of Computational Fluid Mechanics*, *5*(3), 397–405.

Hirt, C. W., & Nichols, B. D. (1981). Volume of fluid (VOF) methods for the dynamics of free boundaries. *Journal of Computational Physique*, *39*, 201–225.

Hodskinson, A., & Ferguson, R. I. (1998). Numerical modelling of separated flow in river bends: Model testing and experimental investigation of geometric controls on the extent of flow separation at the concave bank. *Hydrological Processes*, *12*(8), 1323–1338.

Kindsvater C. E., Carter R. W., Tracy H. J. (1953). Computation of peak discharge at contractions, United State Geological Survey. Circular 284, Washington, DC.

Kocaman, S. (2014). Prediction of backwater profiles due to bridges in a compound channel using CFD. *Advances in Mechanical Engineering*, *6*, 1–9.

Launder, B. E., & Spalding, D. B. (1972). *Mathematical models of turbulence*. London, New York: Academic Press.

Matthai, H. F. (1967). Measurement of peak discharge at width contractions by indirect methods. In *Techniques of water resource investigations of the United States Geological Survey. Applications Hydraulics, Chapter A4, Book 3*. Washington, DC: US Geological Survey (USGS).

Morvan, H., Knight, D., Wright, N., Tang, X., & Crossley, A. (2008). The concept of roughness in fluvial hydraulics and its formulation in 1D, 2D and 3D numerical simulation models. *Journal of Hydraulic Research*, *46*(2), 191–208.

Nichols, B. D., & Hirt, C. W. (1975). Methods for calculating multi-dimensional, transient free surface flows past bodies. In *Proceedings first international conference on numerical ship hydrodynamics*. Bethesda, Md: Naval Ship Research and Development Center, pp. 253–277.

Panattoni, L., & Wallis, J. R. (1979). The Arno River Flood Study (1971–1976). *Eos, Transactions American Geophysical Union*, *60*(1), 1–5.

Principe, P., & Sica, P. (1967). *L'inondazione di Firenze del 4 Novembre 1966 [The November 4th 1966 flooding in Florence]*. Vol. 2, pp. 192–222. L'Universo, Istituto Geografico Militare (in Italian).

Quaranta, E., Katopodis, C., Revelli, R., & Comoglio, C. (2017). Turbulent flow field comparison and related suitability for fish passage of a standard and a simplified low-gradient vertical slot fishway. *River Research and Applications*, *33*(8), 1295–1305.

Settesoldi, D., Paris, E., & Lubello, C. (1996). Verifica idraulica dell'Arno nel tratto urbano fiorentino [Hydraulic simulation in the urban reach of the Arno River]. In *Proceedings, La difesa dalle alluvioni - Convegno Scientifico in occasione del trentennale dell'alluvione di Firenze,* Firenze, pp. 379–392 (in Italian).

Skogerboe G. V., Hyatt M. L., Lloyd A. H. (1967). *Design and calibration of submerged open channel flow measurement structures: Part 4 – Weirs*, Reports of the Utah Water Research Laboratory, Paper 80.

Speziale, C. G., & Thangam, S. (1992). Analysis of an RNG based turbulence model for separated flows. *International Journal of Engineering Science*, *30*(10), 1379–1388.

Tuyen, N. B. (2006). *Flow over oblique weirs. MSc Thesis*. Delft, The Netherlands: Delft University of Technology.

Yakhot, V., & Orszag, S. A. (1986). Renormalization group analysis of turbulence. I. Basic theory. *Journal of Scientific Computing*, *1*(1), 3–51.

Yakhot, V., Orszag, S. A., Thangam, S., Gatski, T. B., & Speziale, C. G. (1992). Development of turbulence models for shear flows by a double expansion technique. *Physics of Fluids A: Fluid Dynamics*, *4*(7), 1510–1520.

How to cite this article: Peruzzi C, Castaldi M, Francalanci S, Solari L. Three-dimensional hydraulic characterisation of the Arno River in Florence. *J Flood Risk Management*. 2019;12 (Suppl. 1): e12490. https://doi.org/10.1111/jfr3.12490